Electronic Supplementary Material (ESI) for Chemical Communications.

Supporting Information

Graphene oxide-wrapped dipotassium terephthalate hollow microrods for enhanced potassium storage

*Xuanpeng Wang‡, Kang Han‡, Chenyang Wang‡, Ziang Liu, Xiaoming Xu, Meng Huang, Ping Hu, Jiashen Meng, Qi Li*and Liqiang Mai**

State Key Laboratory of Advanced Technology for Materials Synthesis and Processing, Wuhan University of Technology, Wuhan 430070, China

Email: qi.li@whut.edu.cn, mlq518@whut.edu.cn

Experimental

Synthesis of hollow microrod K_2TP and bulk K_2TP

The K_2TP was feasibly synthesized with a reflux condensation process referring to literature. In detail, firstly, 22 mmol KOH (AR, 99%) was dissolved in 40 ml deionized water in 20% mass excess, and 10 mmol terephthalic acid (PTA) (Alfa, 98%) was added under the temperature of 50 °C under stirring and then standing the aqueous solution for 8~12 h. Secondly, 100 ml absolute ethanol was added followed by a refluxing process at 90 °C for 12 h. Utilizing ethanol is to precipitate the product and control grain size via decreasing its solubility. Thirdly, the as-obtained precipitate was centrifuged and filtered with ethanol to get rid of surplus alkali. Lastly, hollow microrod K_2TP was obtained by vacuum-drying at 110 °C overnight. The procedure for the synthesis of bulk K_2TP is similar to the synthesis of hollow microrod K_2TP as above. The difference is that 100 ml absolute ethanol was added into the aqueous solution of KOH and PTA after stirring under 50 °C directly without static process.

Synthesis of K_2TP@GO

The K_2TP@GO was simply synthesized as follows: 0.2 g K_2TP was dispersed in 20 ml (10 wt% relative to K_2TP) graphene oxide (GO) aqueous solution (0.5 mg ml^{-1}) under stirring uniformly. The product was obtained by freezing-dry for at least 48 h. We prepared hollow microrods of K_2TP using the neutralization reaction between terephthalic acid and KOH in 50 °C aqueous solution under stirring, and refluxing at 90 °C overnight. Then, K_2TP was added into graphene oxide aqueous solution.

Finally, K_2TP@GO was obtained by freeze-drying the homogeneous solution of graphene oxide and K_2TP.

Characterization

The crystalline structure of the materials was characterized by X-ray diffraction (XRD, D8-Advance, Bruker, Cu Kα radiation, $\lambda = 1.542$ Å) at a scan rate of 40° min^{-1} in the range of 10°–80°. Thermal gravimetric analysis (TGA) was taken on a thermal analyzer (STA 409 PC) from 100 to 800 °C at the heating rate of 10 °C min^{-1} in air. Fourier transform infrared spectrometer (FTIR, Shimadzu, IR Prestige-21) test was operated within the wavenumber range of 1000–3500 cm^{-1}. The morphologies of the materials were conducted by field-emission scanning electron microscopy (FE-SEM, SU8010, 97HITACHI).

In-situ XRD experiment during electrochemical testing of battery was performed on a Bruker D8 Discover X-ray diffractometer with a non-monochromated Cu Kα X-ray source scanned at 2θ ranges of 18 – 33°. For *in-situ* XRD measurement, the electrode was placed right behind an X-ray-transparent beryllium window which also acted as a current collector. The *in-situ* XRD signals were collected using the planar detector in a still mode during the charge/discharge processes, and each pattern took 120 s to acquire.

The electrochemical measurements were carried out by assembling 2016 coin cells, which were assembled in a glove box filled with pure argon gas, using potassium metal (99.5%, Sigma-Aldrich) as both the counter electrode and the reference electrode, a 0.8 M KPF_6 in ethylene glycol dimethyl ether (DME) as electrolyte and a whatman glass microfiber filter (Grade GF/F) as the separator. Anodes were obtained by mixing 60% the as-synthesized active materials (K_2TP@GO or K_2TP), 30% acetylene black, and 10% PVDF (using N-methyl-2-pyrrolidone as solvent). The homogeneous slurry was casted onto Cu foil and dried under a vacuum oven at 60 ºC overnight. The anodes were punched into circle slice with an area of ~0.785 cm^2 and the average electrodes mass loading obtained was about 1.5 - 2.0 mg/cm^{-2}. The electrochemical performance of the cells was tested by a Land Battery Test System with a cut-off voltage range from 0.1 to 2.0 V (*vs.* K/K^+). Cyclic voltammetry (CV) were performed from 0.1 to 2.0 V at a scan rate of 0.1 mV s^{-1} and impedance spectroscopy (EIS) with the amplitude of 10 mV in the frequency range from 100 kHz to 0.01 Hz were measured with a Biologic VMP-3 electrochemical workstation.

Diffusion coefficients of K_2TP@GO and K_2TP

Diffusion coefficients of K_2TP@GO and K_2TP are calculated based on the Randles–Sevcik equation, where Ip is the peak current, n is the number of electrons transferred per molecule during the electrochemical reaction, A is the active surface area of the electrode, C is the concentration of potassium ions in the anode, D is the apparent K^+ diffusion coefficient of the whole electrode involving the diffusion of both potassium ions and electrons, and v is the scanning rate.

$$Ip=0.4463n\,FAC\left(\frac{NFvD}{RT}\right)^{1/2}=2.69\times10^{5}\times n^{3/2}AD^{1/2}Cv^{1/2}$$

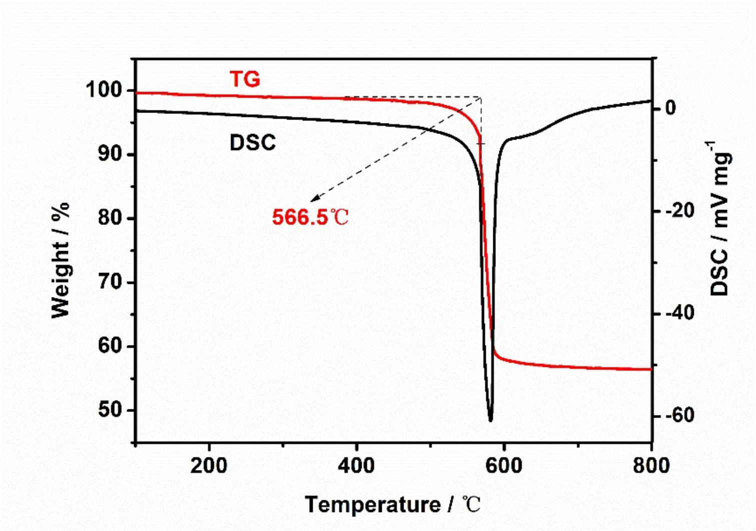

Fig. S1 TGA analysis of as-synthesis K_2TP.

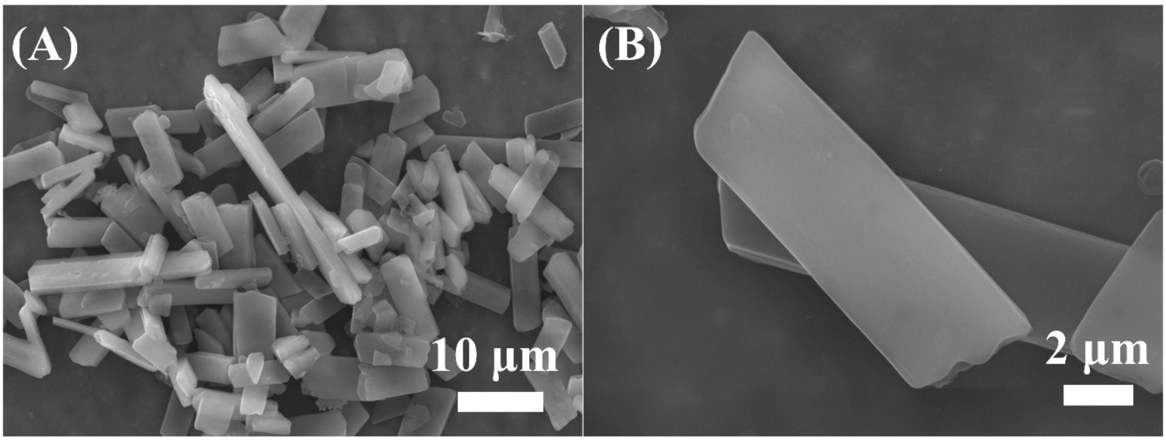

Fig. S2 SEM images bulk K_2TP.

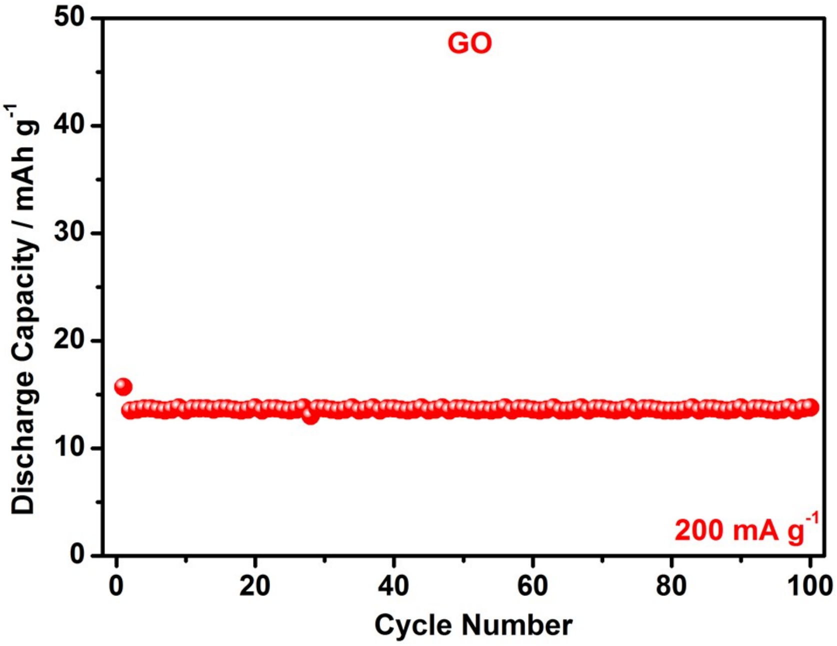

Fig. S3 The storage potassium performance of GO in half cell at current density of 200 mA g^{-1}. The GO electrode exhibits adischarge capacity of ~14.0 mAh g^{-1} at a current density of 200 mA g^{-1}. In addition, due to the low content of GO in the K_2TP@GO composite, the GO contributes to the negligiblecapacity of the K_2TP@GO composite.

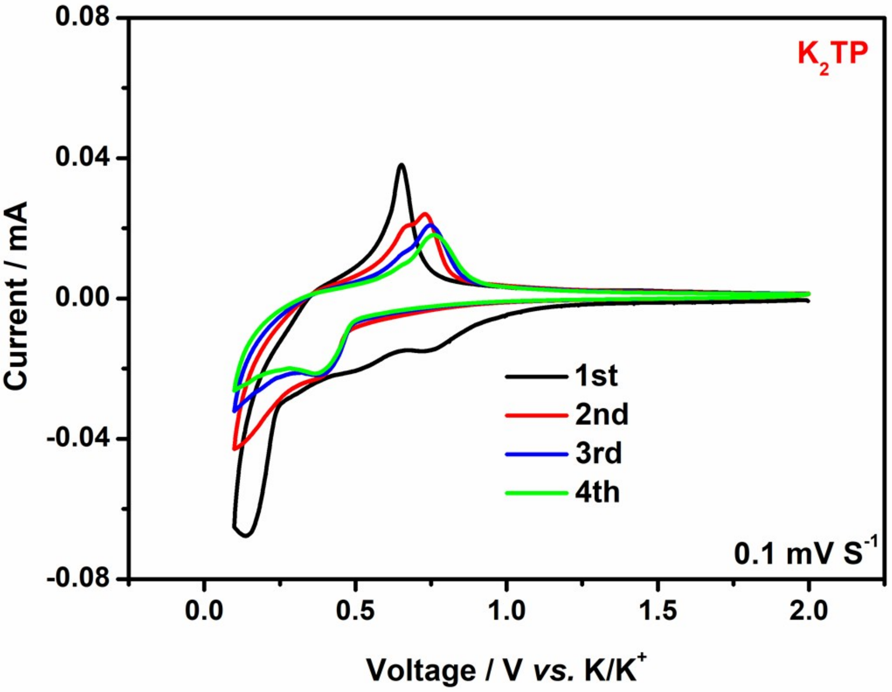

Fig. S4 CV curves of K_2TP in the electrochemical window between 0.1 and 2.0 V at a scan rate of 0.1 mV s^{-1} in the first four cycles.

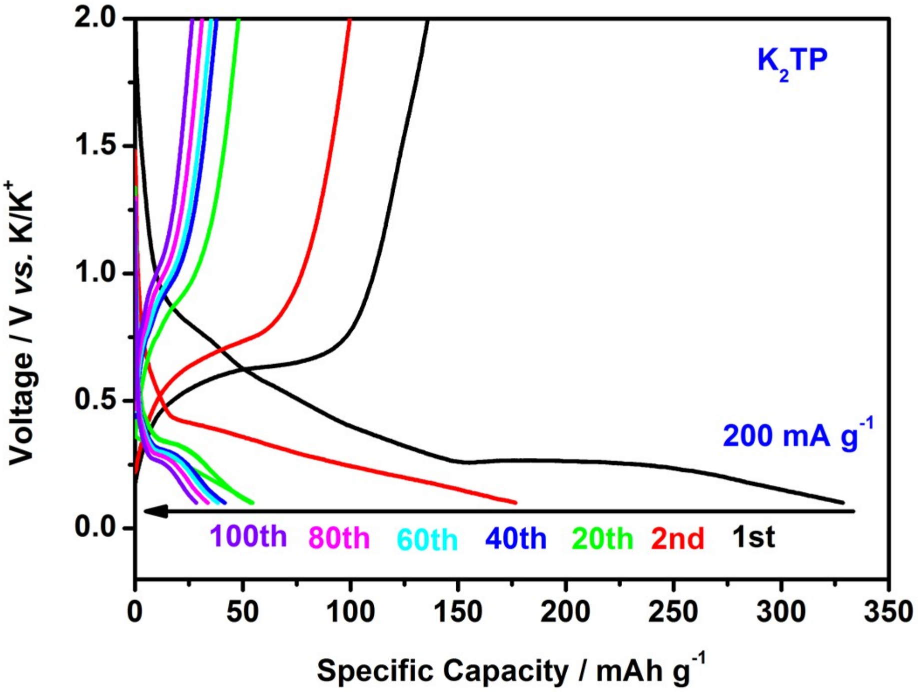

Fig. S5 Charge and discharge curves of K_2TP@GO at the current density of 200 mA g^{-1}.

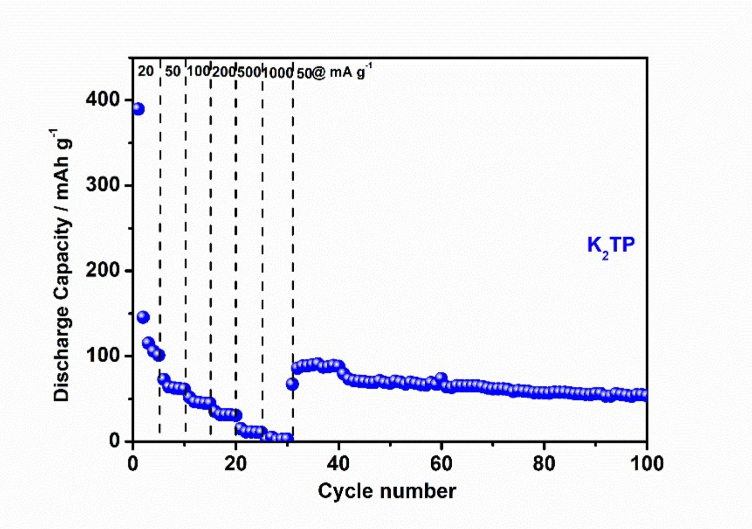

Fig. S6 Rate performance of K_2TP at different rates ranging from 20 to 1000 and back to 50 mA g^{-1}. The rate performance of bulk K_2TP is quite poor as its capacity decreases to almost zero when the current is increased to 1000 mA g^{-1} .

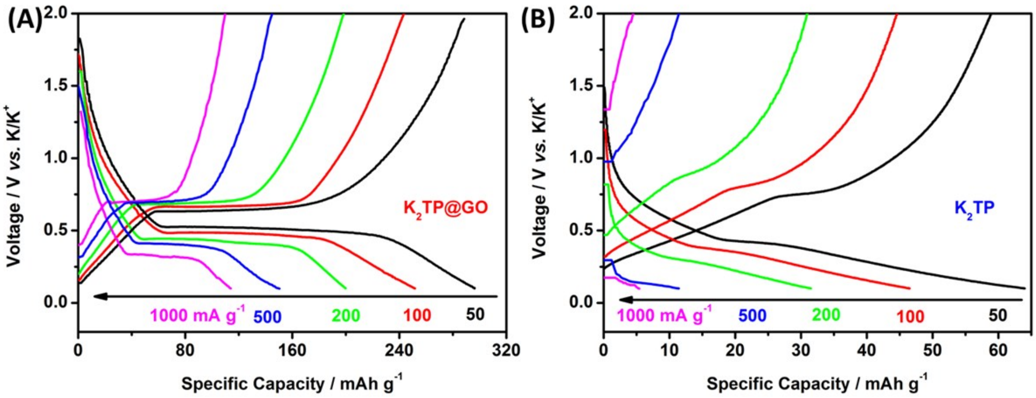

Fig. S7 Charge and discharge curves of K_2TP@GO (A) and K_2TP (B) at different rates ranging from 50 to 1000 and back to 50 mA g^{-1}.

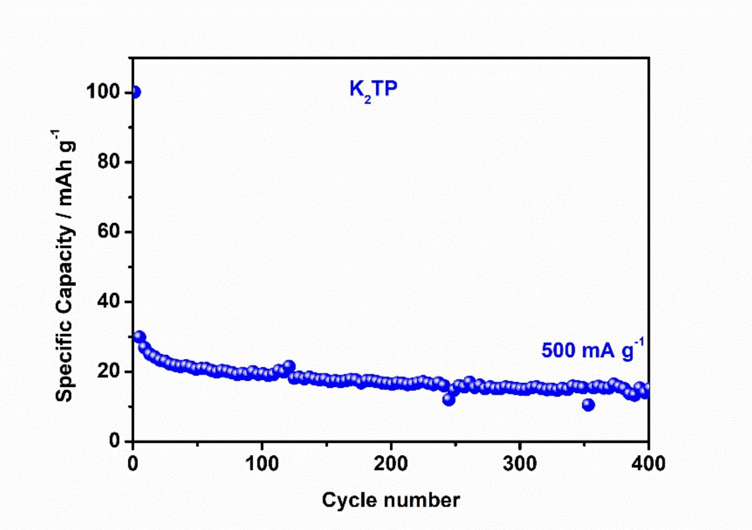

Fig. S8 Cycling measurements of tested at 500 mA g^{-1}.

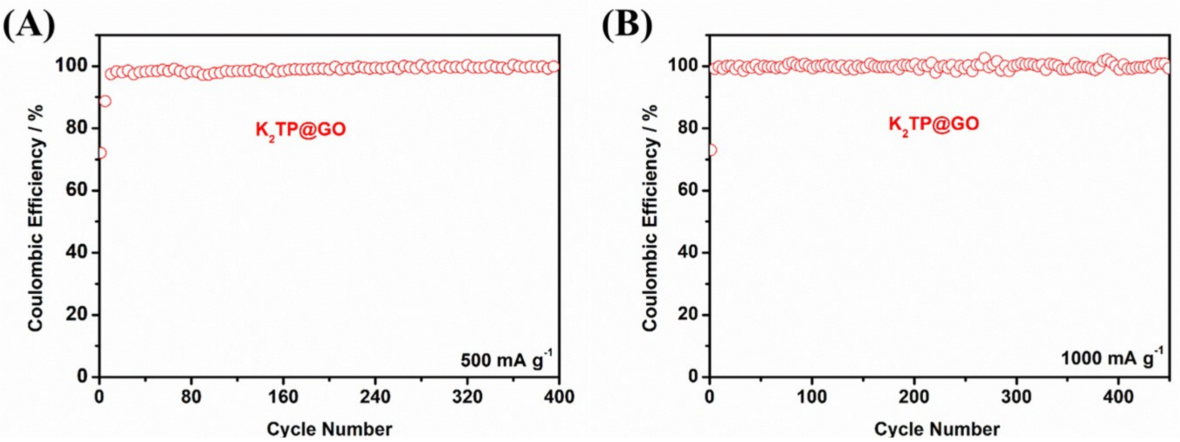

Fig. S9 Coulombic efficiency of K$_2$TP@GO electrode at the current density of 500 and 1000 mA g^{-1}.

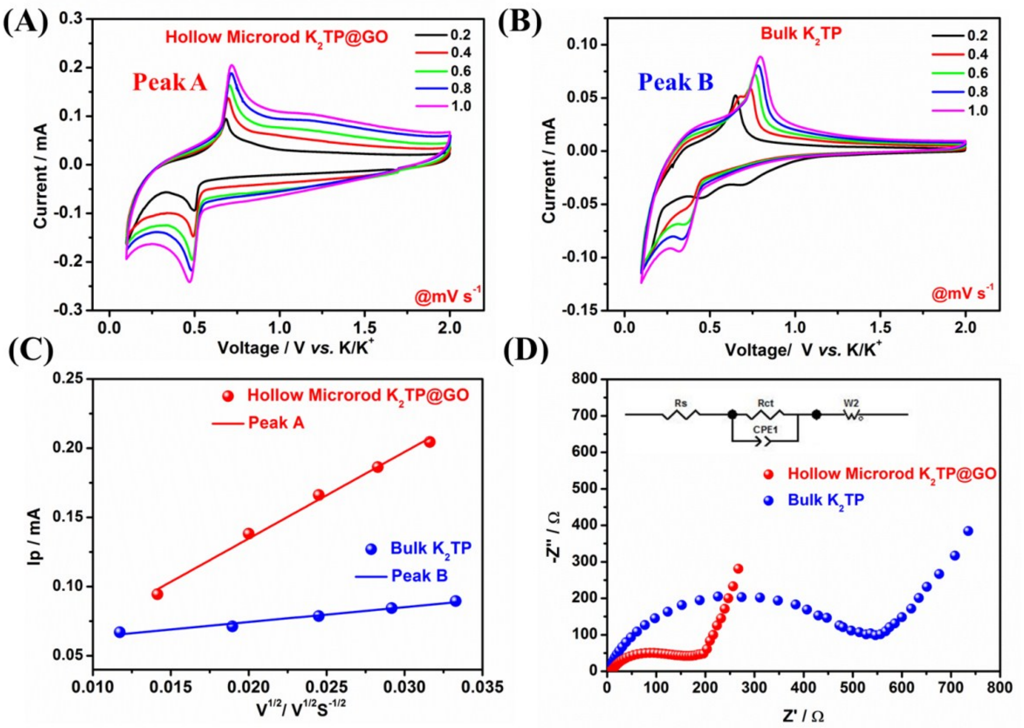

Fig. S10 CV curves of K_2TP@GO (A) and K_2TP (B) at diversity scan rates, and (C) the corresponding relationship between the peak current (Ip) and the square root of scan rate $v^{1/2}$). (D) EIS plots of two electrodes.

To verify the diffusion coefficients of K^+ of K_2TP@GO and bulk K_2TP electrode, CVs tests were conducted at variable scan rates (Fig. S10 A and B). The diffusion coefficients of K^+ are calculated based on the Randles–Sevcik Equation. From the slope of the fitting line collected from the anodic peak A and peak B, the diffusion coefficient of the K_2TP@GO is estimated to be 1.56×10^{-11} cm^2 s^{-1}, which is 8.45 times higher than that of the bulk K_2TP (1.84×10^{-12} cm^2 s^{-1}) (Fig. S10C and D).

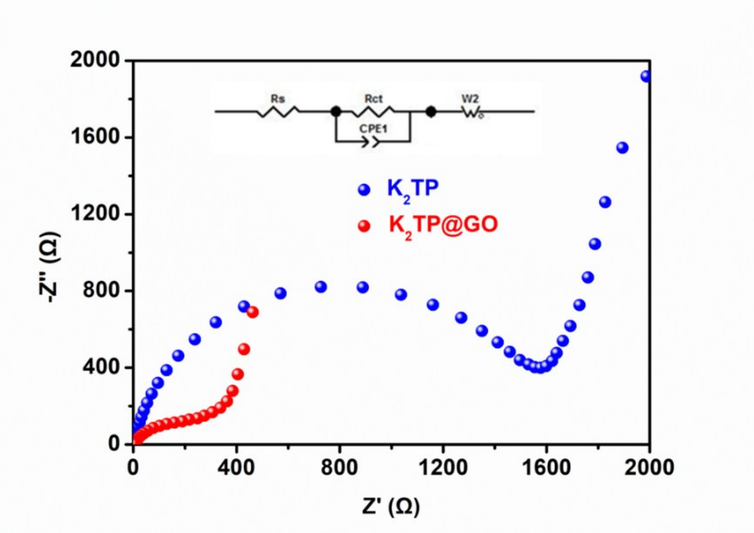

Fig. S11 EIS plots of K_2TP@GO and K_2TP electrodes at different rates ranging after 100 cycles at the current density of 100 mA g^{-1}.

To provide further insights, electrochemical impedance-spectroscopy (EIS) was applied to quantify the resistance at the electrode/electrolyte interface. The results demonstrate a much smaller charge transfer resistance (R_{ct}) of the K_2TP@GO (164.1 Ω) compared to that of bulk K_2TP (544.5 Ω) before cycling, manifesting a superior electron transfer. Apparently, the R_{ct} value of K_2TP@GO still remains much lower than that of bulk K_2TP after 100 cycles at 100 mAh g^{-1}. (Fig. S11). This is because graphene wrapped layer restrains the dissolution as well as accommodates the volume expansion during repeated potassiation/depotassiation processes.

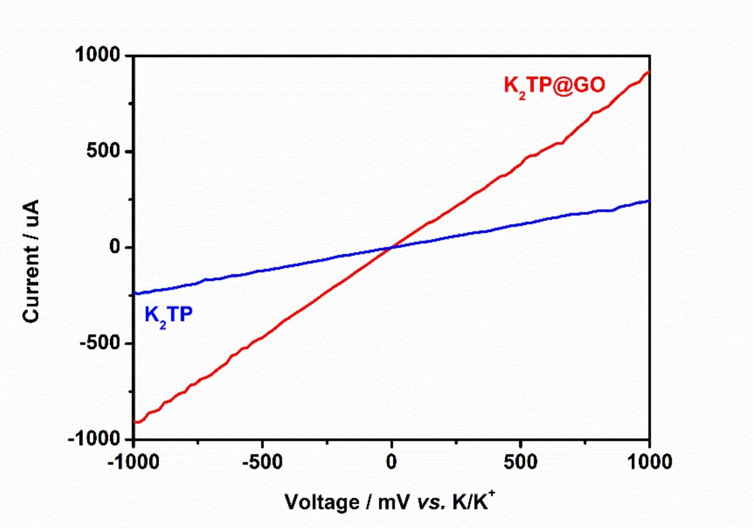

Fig. S12 I−V measurement of K_2TP@GO (A) and K_2TP (B). The I−V measurement shows that the electric conductivity of K_2TP@GO is much more superior to K_2TP.

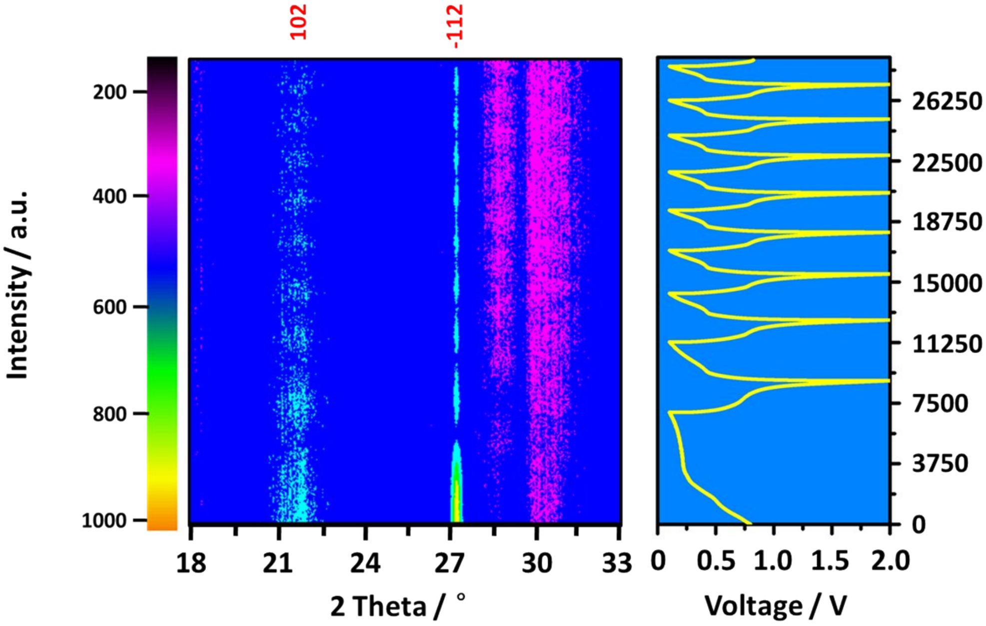

Fig. S13 In-situ XRD patterns of K_2TP@GO electrode during galvanostatic depotassiation/potassiation process at 100 mA g^{-1}. The image plot of the diffraction patterns at 25 – 29.5° during the first three cycles.

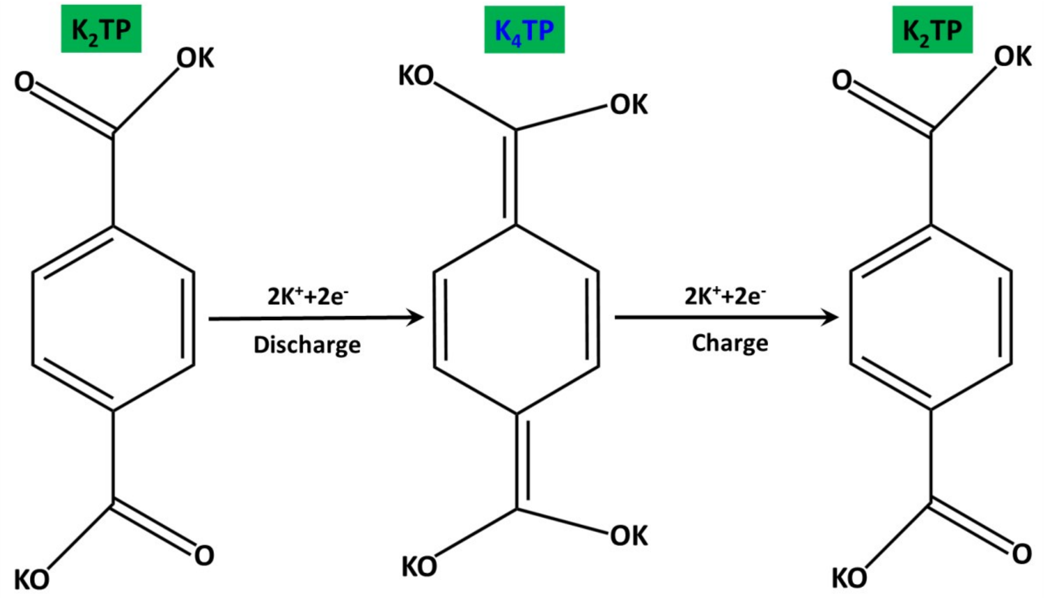

Fig. S14 Schematic illustration of the K^+ insertion/extraction in K_2TP@GO electrode.

Table. S1. Electrochemical performance comparison of various K-ion anodes.

Active materials	Current density (mA g^{-1})	Reversible capacity (mAh g^{-1})	Cycle numbers	Capacity retention	Voltage ranges (V)
K_2TP@GO (This Work)	**200**	**212**	**100**	**91%**	**0.1 – 2.0**
	500	**160**	**400**	**96%**	
	1000	**69**	**450**	**70%**	
K_2TP[S1]	44	181	100	87%	0.1 – 2.0
K_2PC[S1]	44	190	100	93	0.1 – 2.0
K_2BPDC@GO[S2]	50	170	100	91%	0.1 – 2.5
K_2SBDC@GO[S2]	50	124	100	83%	0.1 – 2.5
$K_2C_6O_6$[S3]	300	150	100	60%	0.1 – 3.2
Graphite[S4]	140	100	50	51%	0.01 - 1.5
$K_2Ti_8O_{17}$[S5]	20	111	50	82%	0.1 - 2.0
Sn-C[S6]	25	105	30	64%	0.01-2.0

References

S1. Q. Deng, J. Pei, C. Fan, J. Ma, B. Cao, C. Li, Y. Jin, L. Wang and J. Li, *Nano Energy*, 2017, **33**, 350-355.

S2. C. Li, Q. Deng, H. Tan, C. Wang, C. Fan, J. Pei, B. Cao, Z. Wang and J. Li, *ACS Appl. Mat. Interfaces*, 2017, **9**, 27414-27420.

S3. Q. Zhao, J. Wang, Y. Lu, Y. Li, G. Liang and J. Chen, *Angew. Chem., Int. Ed.*, 2016, **55**, 1-6.

S4. Z. Jian, W. Luo and X. Ji, *J. Mater. Chem. A*, 2015, **137**, 11566-11569.

S5. J. Han, M. Xu, Y. Niu, G. N. Li, M. Wang, Y. Zhang, M. Jia and C. M. Li, *Chem. Commun.*, 2016, **52**, 11274-11276.

S6. I. Sultana, T. Ramireddy, M. M. Rahman, Y. Chen and A. M. Glushenkov, *Chem. Commun.*, 2016, **52**, 9279-9282.